Acta Crystallographica Section C
**Crystal Structure Communications**
ISSN 0108-2701

# Orientational disorder in 4-chloronitrobenzene

**Lynne H. Thomas,[a] Jacqueline M. Cole[a]*‡ and Chick C. Wilson[b]**

[a]Department of Chemistry, University of Cambridge, Lensfield Road, Cambridge CB2 1EW, England, and [b]Department of Chemistry and WestCHEM Research School, University of Glasgow, Glasgow G12 8QQ, Scotland
Correspondence e-mail: jmc61@cam.ac.uk

Received 20 October 2007
Accepted 3 April 2008
Online 26 April 2008

The crystal structure of 4-chloronitrobenzene, $C_6H_4ClNO_2$, a material that exhibits disorder in the solid state, is re-examined using multiple-temperature single-crystal X-ray diffraction. Our results show a marked improvement on previous crystal structure determinations and our comprehensive multiple temperature measurements help to rationalize the structural anomalies. 4-Chloronitrobenzene exhibits twofold orientational disorder of the $NO_2$/Cl substituents, with the molecule lying across an inversion centre. There is also evidence of large thermal motion, which exists at all temperatures and reflects the presence of significant disorder in this material. The nitro group shows possible libration, with one O atom exhibiting larger thermal motion than the other across the whole temperature range. This is explained by a difference in hydrogen-bonding environment.

## Comment

4-Chloronitrobenzene (*p*-ClNB) is one in a series of chloronitrobenzene derivatives that have a disordered structure in their crystalline state. Phase transitions are commonly associated with this disorder in these materials. Furthermore, there appears to be a correlation between this molecular disorder

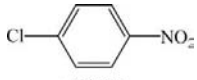


*p*-ClNB

and the unusual dielectric behaviour that this series of materials tend to exhibit (Hall & Horsfall, 1973; Tanaka *et al.*, 1974; Khotsyanova *et al.*, 1969; Sakurai, 1962). Hitherto, three attempts to determine the crystal structure of *p*-ClNB have been made.

An initial indication of the nature of the crystal structure of *p*-ClNB was given by Toussaint (1952), who postulated that the space group could be $P2_1/c$ with $Z = 2$ and a disordered crystal structure, or $Pc$ with an ordered structure. It was concluded that $Pc$ was more likely than $P2_1/c$.

A subsequent study of *p*-ClNB at room temperature (Mak & Trotter, 1962) revealed that the crystal structure was disordered over two possible orientations. The resulting disordered model, once refined, yielded $R = 0.23$ in the [100] projection and $R = 0.26$ in the [010] projection. An accurate determination of the bond geometry was not possible because of the disorder. However, basic analysis of intermolecular separations was able to show that all such separations corresponded to expected sums of relevant van der Waals radii. This implied that the two disordered orientations existed in the crystal structure without any steric or electronic hindrance. The fact that no diffuse scattering was observed in the measurements also led to the conclusion that the two possible disordered orientations were randomly positioned throughout the crystal structure.

More recently, a third attempt was made to reveal the nature of disorder in *p*-ClNB (Meriles *et al.*, 2000). This study employed powder X-ray diffraction at a range of temperatures. Meriles *et al.* determined that a first-order phase transition exists in *p*-ClNB at 282 K. Above this temperature, the crystal structure was found to be disordered, as determined by Mak & Trotter (1962). At temperatures below 282 K, the powder study indicated an ordered structure in space group $P2_1$ ($Z = 2$). It is worthy of note that the crystal structure of the ordered phase was derived from a sample that had been stored cryogenically at 250 K for three months prior to the experiment. Such storage conditions were deemed necessary in order to ensure complete transformation to the ordered phase. Furthermore, a much higher level of background, present with a marked modulated profile, was noted in the diffraction pattern of this disordered phase compared with the low background associated with data from the ordered structure. This was attributed to diffuse scattering caused by molecular disorder.

Previously, nuclear quadrupolar resonance (NQR) had also been used to investigate this disorder on a local scale, with somewhat contradictory results (Meriles *et al.*, 1996, 1997; González & Pusiol, 1996). In light of the limitations of the powder diffraction study and the uncertainties observed in the various NQR spectroscopy studies, the molecular disorder in *p*-ClNB has now been reinvestigated using multi-temperature single-crystal X-ray diffraction.

We were interested in exploring changes in the structure as a function of temperature. Data were therefore collected at 260, 250, 240, 230, 200, 150 and 100 K, and then again at 260 K to check for any hysteresis effects. The crystal was also observed to show a significant degree of sublimation at 270 K, making it difficult to collect data at this temperature. Subsequent thermogravimetric analysis indicated that a sample the size of that used would diminish to around 10% of its initial volume in 50 min when held at 310 K, confirming its propensity to sublimation. The crystal structure solves to a twofold

‡ Permanent address: Department of Physics, Cavendish Laboratory, University of Cambridge, J. J. Thomson Avenue, Cambridge CB3 0HE, England.

  doi:10.1107/S0108270108008998 

orientationally disordered model, with the molecule lying across an inversion centre, as shown in Fig. 1. As it is the most accurate available determination, the 100 K structure is discussed further.

Owing to the molecular disorder, the Cl and N atomic fractions on each substituent site lie very close to one another in the model, resulting in a severe overlap of electron-density contributions to scattering on each site. This proximity, combined with the fact that Cl possesses a much higher electron density, makes it difficult to determine accurately the position of the N atom (and hence to draw any conclusions on its thermal motion, *vide infra*). Fourier maps calculated in the region of the $NO_2$/Cl groups, however, clearly confirm the presence of both groups on this site (Fig. 2).

The difficulty in assigning the electron density associated with the N and Cl atoms due to the presence of the disorder results in the apparent C—Cl distance from the refinement being longer than expected [1.903 (3) Å at 100 K], whilst the apparent C—N distance is shorter than expected [1.330 (6) Å at 100 K]. The mean C—Cl distance in the Cambridge Structural Database (CSD; Allen, 2002; Bruno *et al.*, 2002) for a Cl atom bonded to a benzene ring is 1.734 Å, the total range of values present being between 1.592 and 1.789 Å. The value found here is outside that range. The mean N—C bond length for an N atom within a nitro group bonded to a benzene ring is 1.467 Å, and the range found in the CSD is 1.396–1.544 Å. Again, the observed value for the unconstrained refinement here lies outside of this range. These bond lengths could be explained by consideration of the displacement ellipsoids of the C atoms in the benzene ring, as they are all elongated in the direction of the Cl atom/$NO_2$ group (Fig. 1). This elongation could be interpreted in terms of the presence of two positions on each lattice point shifted relative to one another depending on the orientation of the molecule. The N atom is also located slightly off-centre, and thus one N—O bond length is considerably shorter than the other, with asymmetric O—N—C bond angles. The electron density associated with the O atoms is well defined and isolated from any other atoms, as shown in the difference Fourier maps (Fig. 2), and thus their positions could be considered to be more certain than the position of the N atom, whose electron density is located close to that of the Cl atom.

In light of these abnormal bond lengths, a series of restraints and constraints were applied to the refinement to augment the

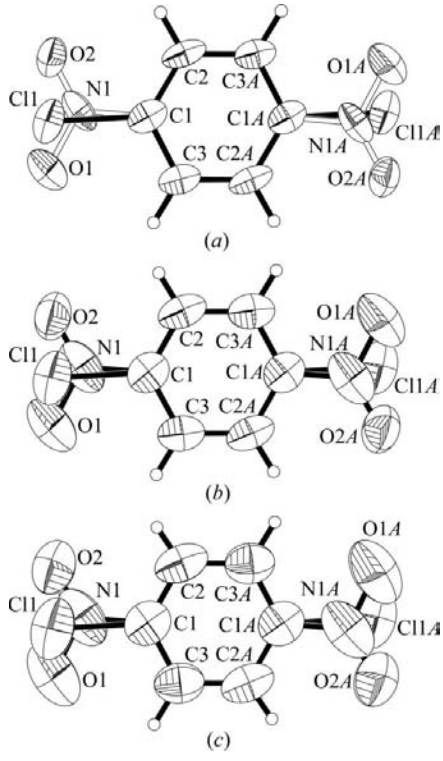


**Figure 1**
The disorder in *p*-ClNB at (*a*) 100 K, (*b*) 200 K and (*c*) 260 K. Displacement ellipsoids are plotted at the 50% probability level.

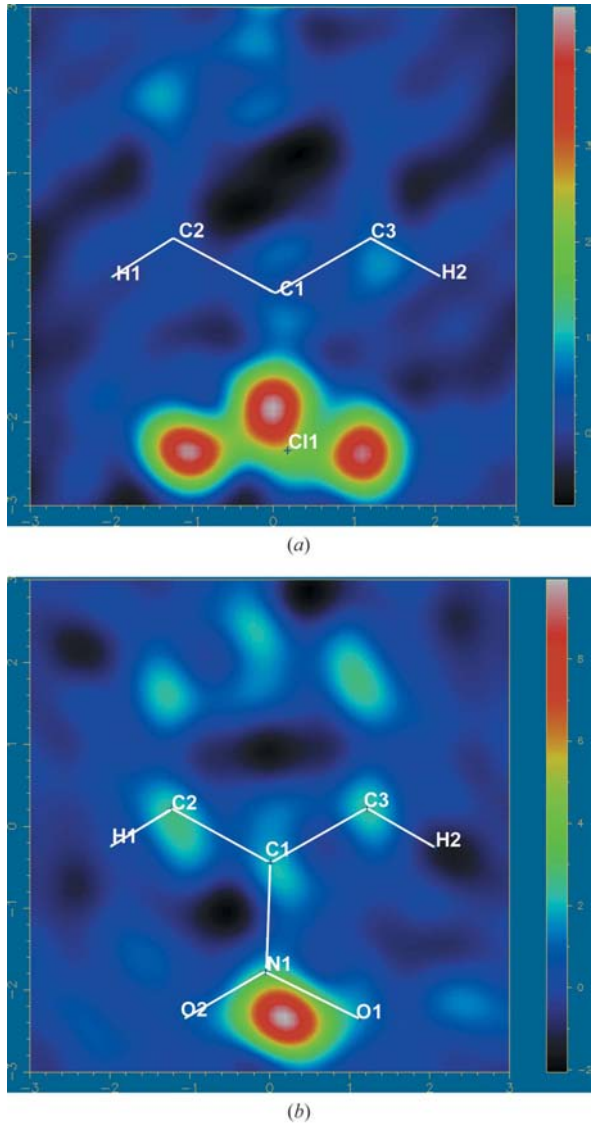


**Figure 2**
(*a*) A difference Fourier image showing the $NO_2$ group (calculated using a model with $NO_2$ removed) and (*b*) an $F_{obs}$ image of the Cl atom in the structure of *p*-ClNB at 100 K. (Areas of high electron density are red in the electronic version of the paper and areas of low electron density are blue.)

initial unconstrained refinement and the visual information from the difference Fourier maps. Initially, the O—N bond lengths were restrained to take the same value; this geometry would be expected in a disorder-free symmetric nitro group (Fig. 3*a*). This restraint resulted in an increase in the *R* factor at 100 K from 0.0456 to 0.0464. The effect of applying this restraint is to equalize the N—O bond distances somewhat, but at the expense of shortening the N—C bond length further (Table 8). A stronger restraint could be applied, but this resulted in a further rise in the *R* factor and a further shortening of the N—C bond length, although it does force the O—N bond lengths to be equivalent and the O—N—C angles to be more similar (Fig. 3*b*). Application of the equivalent similarity restraints for the O—N—C angles resulted in similar effects. A refinement was also attempted to force the C—Cl and C—N bond lengths to take more conventional values (1.74 and 1.47 Å, respectively). This has the effect of reducing the N—O bond lengths to values shorter than those reported in the CSD (Bruno *et al.*, 2002), but the values of the N—O distances and O—N—C angles are more symmetric. However, there is a significant rise in the *R* factor, and the difference Fourier map arising from the model clearly shows excess electron density around both the Cl and the N atoms, and some areas where too much electron density has been allocated (Fig. 3*c*). The anisotropic atomic displacement parameters also become extremely elongated, suggesting that this is not a good model. Fixing the N—O bond lengths to a more conventional value of 1.221 Å caused the *R* factor to rise to 0.0480 (Fig. 3*d*). However, the N—O bond lengths become relatively similar, as do the O—N—C bond angles. The N—C bond length is shorter than that found in the freely refined case, and the C—Cl bond length is slightly longer. This approach perhaps provides the best model for the molecule, as the nitro group is forced to adopt a more regular geometry. The model is still limited in the sense that it fails to deal adequately with the abnormal N—C and Cl—C bond lengths. This may suggest that the disorder is not simply a case of the molecule being flipped about a central point; rather, there is some translational component in the superposition of the two molecular orientations. Attempts were made to refine the structure in $P2_1$, but these gave a poorer agreement while not affecting the refined occupancies; $P2_1/c$ appears to be the most appropriate space group for this refinement.

The average structure reveals two contacts that are shorter than the sum of the van der Waals radii (VDW). The first creates a dimer unit with a close O···H distance of 2.47 (2) Å

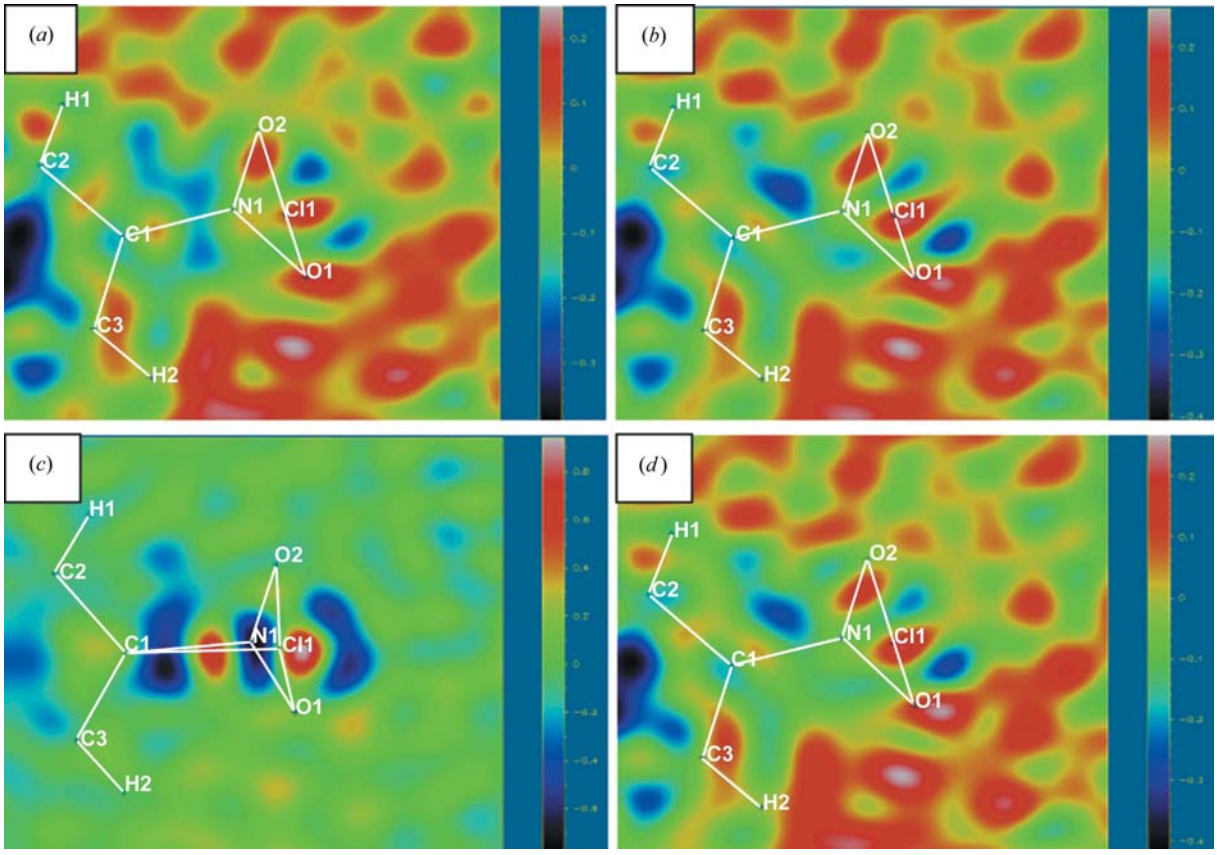


**Figure 3**
Fourier difference maps for the restrained and constrained models, with all atoms defined in the structure. (*a*) The restrained N—O bond lengths with 0.02 Å standard deviation, (*b*) the restrained N—O bond lengths with 0.002 Å standard deviation, (*c*) the case where the Cl—C and N—C bond lengths are forced to be close to their standard values, and (*d*) the case where the N—O bond lengths are constrained to be close to their standard values. The Fourier difference maps for (*a*), (*b*) and (*d*) are similar. The Fourier difference map for (*c*) clearly shows the unaccounted and over-accounted for electron density. (Areas of high electron density are red in the electronic version of the paper and areas of low electron density are blue.)

at 100 K (VDW = 2.72 Å), and the second, a close O···Cl contact of 3.112 (4) Å (VDW = 3.27 Å). The dimers are not quite coplanar (Fig. 4). The O···Cl contact lies approximately along the line of the C—Cl bond (Fig. 5).

In general, the thermal motion of *p*-ClNB (Fig. 1) appears to be large at all temperatures (*e.g.* Table 9). It is possible that there is complex static disorder present, where two possible orientations that do not entirely overlap are translationally displaced from one another. It is not possible to reach any firm conclusions regarding this hypothesis using standard Bragg scattering techniques; instead, modelling of diffuse scattering can yield information on this (*e.g.* Thomas *et al.*, 2007). The most significant thermal motion of the $NO_2$ group is observed in $U_{33}$. The aforementioned problems associated with spatial overlap of the electron density of the N and Cl atoms may place some limitations on the accuracy of the atomic positions for these atoms (Fig. 2). However, atom O1 is found to be librating more than atom O2. This may be explained by considering the number of close intermolecular contacts in the packing of the molecules (Tables 1–7). Atom O1 is involved in a weak hydrogen bond (Desiraju & Steiner, 2001), where the interatomic distance [2.47 (2) Å] is less than the sum of the van der Waals radii of the two atoms (2.72 Å) (Fig. 4). Atom O2 has a close interatomic contact between the O and H atoms that is on the limit of the sum of the van der Waals radii [2.68 (2) Å]. There is also a close Cl···O intermolecular contact [3.112 (4) Å] involving atom O2 (Fig. 5). These interactions may place restrictions on the freedom of atom O2 to librate relative to that of O1, which may lead to the enhanced motion of one relative to the other.

Whilst no crystallographic phase transition was found in the temperature range 100–260 K, the possible drop in the cell parameter *b* (and possibly in *c*) at temperatures higher than 250 K (Fig. 6) hints at an incipient phase transition in this temperature region. This observation could relate to the phase transition revealed by Meriles *et al.* (2000), though there is a temperature mismatch. Analysis of $U_{ii}$ as a function of temperature also shows nitrogen to behave slightly anomalously upon cooling, in the temperature region 230–250 K, though this effect can be complicated in this case because of the disorder present. We could not collect a corresponding single-crystal data set for this material at temperatures above 282 K, however, since we observed that the sample sublimed before a full data set could be collected.

In conclusion, the crystal structure of *p*-ClNB has been studied at multiple temperatures to investigate the possibility of a phase transition at low temperature. The structure was found to be the same at all the temperatures studied, with the orientational disorder persisting at least down to 100 K; the refined disordered structure is of far higher quality than that obtained previously. The freely refined structure finds the O—N bond lengths to be asymmetric, and the N—C and Cl—C distances to be shorter and longer, respectively, than would be expected. The application of a series of restraints and constraints addressed the asymmetry of the N—O bond lengths but at the expense of perturbing the Cl—C and N—C bond lengths. This result potentially highlights a translational component to the disorder. The material shows significant thermal motion, but hydrogen bonding places restrictions on the movement of one O atom relative to the other, resulting in

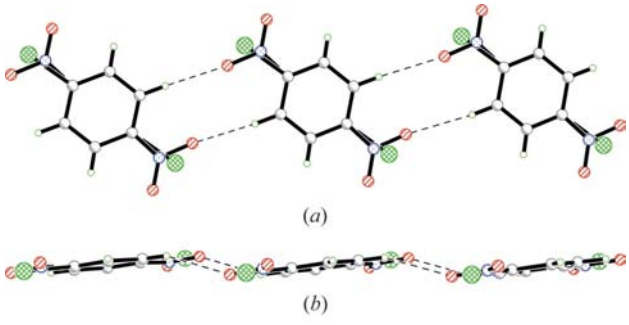


**Figure 4**
The shortest hydrogen bonds in *p*-ClNB. (*a*) The chains of molecules connected by hydrogen bonds. Hydrogen bonding is shown with dashed lines. (*b*) The near-coplanar arrangement of the molecules.

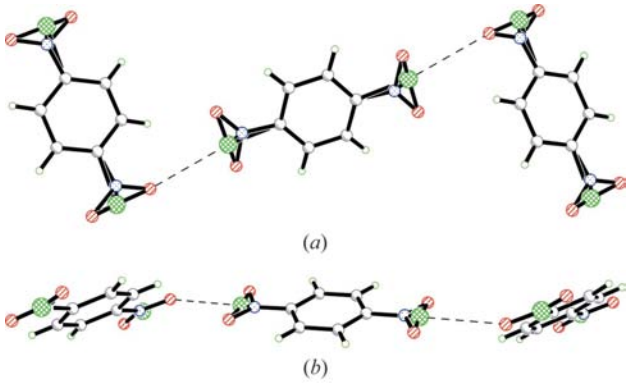


**Figure 5**
(*a*) The Cl···O close contacts between molecules in *p*-ClNB. (*b*) The nonplanar nature of the related molecules, with Cl···O intermolecular interactions represented by dashed lines. Adjacent molecules are related by the symmetry operation $(-x, y+\frac{1}{2}, -z+\frac{1}{2})$.

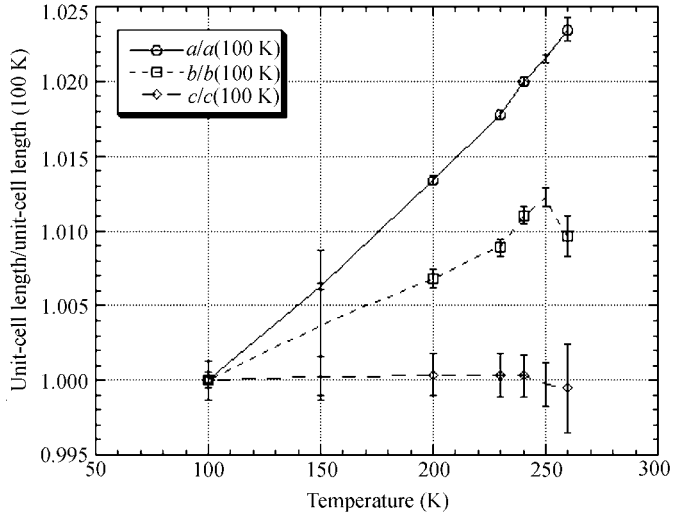


**Figure 6**
Unit-cell lengths of *p*-ClNB, normalized as length/(length at 100 K), as a function of temperature.

an asymmetric libration of the nitro group. It is noted that the displacement ellipsoid model does not provide a comprehensive description of the possible libration of the $NO_2$ group of this compound. This fact suggests that a different modelling technique may be needed to understand better the thermal motion and possible libration observed. In this regard, total scattering studies of this material are in progress, since an analysis of both diffuse and Bragg scattering should also allow us to understand more fully the nature of the disorder; in particular, if there is a latent dynamic component of the disorder or a static translational shift in the positions of the two orientations. Indeed, structured diffuse scattering has already been observed in the diffraction pattern of *p*-ClNB (Thomas, 2007). These more sophisticated disorder models will be constructed using techniques similar to those in a study of the related compound pentachloronitrobenzene (Thomas *et al.*, 2007).

## Experimental

A single crystal of *p*-ClNB was grown from diethyl ether by slow evaporation at room temperature. Data were collected at 100, 150, 200, 230, 240, 250 and 260 K to check for any signs of a phase transition. Attempts were also made to collect data at room temperature but the crystal sublimed before a full data set could be collected. An open-flow nitrogen Oxford Cryosystems cryostream cooler was used for the multiple-temperature measurements.

### *p*-ClNB at all temperatures

*Crystal data*

$C_6H_4ClNO_2$
$M_r$ = 157.55
Monoclinic, $P2_1/c$
$Z$ = 2
Mo $K\alpha$ radiation
0.4 × 0.16 × 0.1 mm

### *p*-ClNB at 260 K

*Crystal data*

$a$ = 3.8011 (8) Å
$b$ = 6.7639 (14) Å
$c$ = 13.364 (3) Å
$\beta$ = 96.82 (3)°
$V$ = 341.17 (12) Å$^3$
$\mu$ = 0.49 mm$^{-1}$
$T$ = 260 (2) K

*Data collection*

Nonius KappaCCD diffractometer
Absorption correction: multi-scan (*SORTAV*; Blessing, 1995)
$T_{min}$ = 0.842, $T_{max}$ = 0.952
2014 measured reflections
730 independent reflections
365 reflections with $I > 2\sigma(I)$
$R_{int}$ = 0.040

*Refinement*

$R[F^2 > 2\sigma(F^2)]$ = 0.046
$wR(F^2)$ = 0.134
$S$ = 1.04
730 reflections
72 parameters
All H-atom parameters refined
$\Delta\rho_{max}$ = 0.17 e Å$^{-3}$
$\Delta\rho_{min}$ = −0.20 e Å$^{-3}$

### *p*-ClNB at 250 K

*Crystal data*

$a$ = 3.7938 (3) Å
$b$ = 6.7564 (6) Å
$c$ = 13.3672 (15) Å
$\beta$ = 96.639 (3)°
$V$ = 340.34 (6) Å$^3$
$\mu$ = 0.49 mm$^{-1}$
$T$ = 250 (2) K

*Data collection*

Nonius KappaCCD diffractometer
Absorption correction: multi-scan (*SORTAV*; Blessing, 1995)
$T_{min}$ = 0.844, $T_{max}$ = 0.944
2071 measured reflections
748 independent reflections
385 reflections with $I > 2\sigma(I)$
$R_{int}$ = 0.037

*Refinement*

$R[F^2 > 2\sigma(F^2)]$ = 0.052
$wR(F^2)$ = 0.139
$S$ = 1.08
748 reflections
72 parameters
All H-atom parameters refined
$\Delta\rho_{max}$ = 0.13 e Å$^{-3}$
$\Delta\rho_{min}$ = −0.15 e Å$^{-3}$

**Table 1**
Hydrogen-bond geometry (Å, °) for *p*-ClNB at 260 K.

| $D$—H···$A$ | $D$—H | H···$A$ | $D$···$A$ | $D$—H···$A$ |
|---|---|---|---|---|
| C3—H2···O1$^{i}$ | 0.97 (3) | 2.58 (3) | 3.493 (8) | 157 (2) |
| C2—H1···O2$^{ii}$ | 0.87 (3) | 2.80 (2) | 3.374 (6) | 125.3 (19) |

Symmetry codes: (i) $-x, -y+1, -z+1$; (ii) $-x+1, y-\frac{1}{2}, -z+\frac{1}{2}$.

**Table 2**
Hydrogen-bond geometry (Å, °) for *p*-ClNB at 250 K.

| $D$—H···$A$ | $D$—H | H···$A$ | $D$···$A$ | $D$—H···$A$ |
|---|---|---|---|---|
| C3—H2···O1$^{i}$ | 0.97 (3) | 2.56 (3) | 3.482 (7) | 158 (2) |
| C2—H1···O2$^{ii}$ | 0.86 (3) | 2.82 (3) | 3.384 (6) | 124.9 (19) |

Symmetry codes: (i) $-x, -y+1, -z+1$; (ii) $-x+1, y-\frac{1}{2}, -z+\frac{1}{2}$.

### *p*-ClNB at 240 K

*Crystal data*

$a$ = 3.7880 (3) Å
$b$ = 6.7482 (6) Å
$c$ = 13.3755 (14) Å
$\beta$ = 96.47 (3)°
$V$ = 339.73 (5) Å$^3$
$\mu$ = 0.49 mm$^{-1}$
$T$ = 240 (2) K

*Data collection*

Nonius KappaCCD diffractometer
Absorption correction: multi-scan (*SORTAV*; Blessing, 1995)
$T_{min}$ = 0.850, $T_{max}$ = 0.945
2069 measured reflections
747 independent reflections
390 reflections with $I > 2\sigma(I)$
$R_{int}$ = 0.046

*Refinement*

$R[F^2 > 2\sigma(F^2)]$ = 0.045
$wR(F^2)$ = 0.122
$S$ = 1.04
747 reflections
72 parameters
All H-atom parameters refined
$\Delta\rho_{max}$ = 0.16 e Å$^{-3}$
$\Delta\rho_{min}$ = −0.20 e Å$^{-3}$

### *p*-ClNB at 230 K

*Crystal data*

$a$ = 3.7801 (3) Å
$b$ = 6.7338 (6) Å
$c$ = 13.3758 (15) Å
$\beta$ = 96.34 (3)°
$V$ = 338.39 (6) Å$^3$
$\mu$ = 0.49 mm$^{-1}$
$T$ = 230 (2) K

*Data collection*

Nonius KappaCCD diffractometer
Absorption correction: multi-scan (*SORTAV*; Blessing, 1995)
$T_{min}$ = 0.857, $T_{max}$ = 0.943
1934 measured reflections
719 independent reflections
396 reflections with $I > 2\sigma(I)$
$R_{int}$ = 0.049

*Refinement*

| | |
|---|---|
| $R[F^2 > 2\sigma(F^2)] = 0.049$ | 72 parameters |
| $wR(F^2) = 0.126$ | All H-atom parameters refined |
| $S = 1.06$ | $\Delta\rho_{max} = 0.21$ e Å$^{-3}$ |
| 719 reflections | $\Delta\rho_{min} = -0.25$ e Å$^{-3}$ |

**Table 3**
Hydrogen-bond geometry (Å, °) for *p*-ClNB at 240 K.

| $D$—H···$A$ | $D$—H | H···$A$ | $D$···$A$ | $D$—H···$A$ |
|---|---|---|---|---|
| C3—H2···O1$^{i}$ | 0.98 (2) | 2.54 (3) | 3.476 (6) | 158.6 (19) |
| C2—H1···O2$^{ii}$ | 0.93 (2) | 2.75 (2) | 3.376 (5) | 126.0 (15) |

Symmetry codes: (i) $-x, -y+1, -z+1$; (ii) $-x+1, y-\frac{1}{2}, -z+\frac{1}{2}$.

**Table 4**
Hydrogen-bond geometry (Å, °) for *p*-ClNB at 230 K.

| $D$—H···$A$ | $D$—H | H···$A$ | $D$···$A$ | $D$—H···$A$ |
|---|---|---|---|---|
| C3—H2···O1$^{i}$ | 0.98 (3) | 2.53 (3) | 3.455 (7) | 158 (2) |
| C2—H1···O2$^{ii}$ | 0.87 (2) | 2.77 (2) | 3.372 (5) | 127.4 (18) |

Symmetry codes: (i) $-x, -y+1, -z+1$; (ii) $-x+1, y-\frac{1}{2}, -z+\frac{1}{2}$.

## *p*-ClNB at 200 K

*Crystal data*

| | |
|---|---|
| $a = 3.7635$ (3) Å | $V = 336.37$ (5) Å$^3$ |
| $b = 6.7201$ (6) Å | $\mu = 0.50$ mm$^{-1}$ |
| $c = 13.3762$ (14) Å | $T = 200$ (2) K |
| $\beta = 96.13$ (3)° | |

*Data collection*

| | |
|---|---|
| Nonius KappaCCD diffractometer | 2051 measured reflections |
| Absorption correction: multi-scan (*SORTAV*; Blessing, 1995) | 736 independent reflections |
| | 448 reflections with $I > 2\sigma(I)$ |
| $T_{min} = 0.838$, $T_{max} = 0.946$ | $R_{int} = 0.046$ |

*Refinement*

| | |
|---|---|
| $R[F^2 > 2\sigma(F^2)] = 0.047$ | 72 parameters |
| $wR(F^2) = 0.119$ | All H-atom parameters refined |
| $S = 1.07$ | $\Delta\rho_{max} = 0.15$ e Å$^{-3}$ |
| 736 reflections | $\Delta\rho_{min} = -0.26$ e Å$^{-3}$ |

**Table 5**
Hydrogen-bond geometry (Å, °) for *p*-ClNB at 200 K.

| $D$—H···$A$ | $D$—H | H···$A$ | $D$···$A$ | $D$—H···$A$ |
|---|---|---|---|---|
| C3—H2···O1$^{i}$ | 0.95 (2) | 2.55 (2) | 3.440 (6) | 156.0 (18) |
| C2—H1···O2$^{ii}$ | 0.89 (2) | 2.74 (2) | 3.363 (5) | 128.1 (16) |

Symmetry codes: (i) $-x, -y+1, -z+1$; (ii) $-x+1, y-\frac{1}{2}, -z+\frac{1}{2}$.

## *p*-ClNB at 150 K

*Crystal data*

| | |
|---|---|
| $a = 3.7372$ (2) Å | $V = 332.47$ (4) Å$^3$ |
| $b = 6.6991$ (5) Å | $\mu = 0.50$ mm$^{-1}$ |
| $c = 13.3748$ (13) Å | $T = 150$ (2) K |
| $\beta = 96.84$ (3)° | |

*Data collection*

| | |
|---|---|
| Nonius KappaCCD diffractometer | 2046 measured reflections |
| Absorption correction: multi-scan (*SORTAV*; Blessing, 1995) | 734 independent reflections |
| | 490 reflections with $I > 2\sigma(I)$ |
| $T_{min} = 0.864$, $T_{max} = 0.946$ | $R_{int} = 0.042$ |

*Refinement*

| | |
|---|---|
| $R[F^2 > 2\sigma(F^2)] = 0.046$ | 72 parameters |
| $wR(F^2) = 0.113$ | All H-atom parameters refined |
| $S = 1.08$ | $\Delta\rho_{max} = 0.17$ e Å$^{-3}$ |
| 734 reflections | $\Delta\rho_{min} = -0.22$ e Å$^{-3}$ |

**Table 6**
Hydrogen-bond geometry (Å, °) for *p*-ClNB at 150 K.

| $D$—H···$A$ | $D$—H | H···$A$ | $D$···$A$ | $D$—H···$A$ |
|---|---|---|---|---|
| C3—H2···O1$^{i}$ | 0.98 (2) | 2.49 (2) | 3.417 (5) | 157.5 (17) |
| C2—H1···O2$^{ii}$ | 0.91 (2) | 2.72 (2) | 3.356 (4) | 128.3 (16) |

Symmetry codes: (i) $-x, -y+1, -z+1$; (ii) $-x+1, y-\frac{1}{2}, -z+\frac{1}{2}$.

## *p*-ClNB at 100 K

*Crystal data*

| | |
|---|---|
| $a = 3.7139$ (2) Å | $V = 329.93$ (4) Å$^3$ |
| $b = 6.6746$ (5) Å | $\mu = 0.51$ mm$^{-1}$ |
| $c = 13.3712$ (13) Å | $T = 100$ (2) K |
| $\beta = 95.49$ (3)° | |

*Data collection*

| | |
|---|---|
| Nonius KappaCCD diffractometer | 2151 measured reflections |
| Absorption correction: multi-scan (*SORTAV*; Blessing, 1995) | 745 independent reflections |
| | 534 reflections with $I > 2\sigma(I)$ |
| $T_{min} = 0.860$, $T_{max} = 0.942$ | $R_{int} = 0.042$ |

*Refinement*

| | |
|---|---|
| $R[F^2 > 2\sigma(F^2)] = 0.046$ | 72 parameters |
| $wR(F^2) = 0.106$ | All H-atom parameters refined |
| $S = 1.12$ | $\Delta\rho_{max} = 0.19$ e Å$^{-3}$ |
| 745 reflections | $\Delta\rho_{min} = -0.30$ e Å$^{-3}$ |

**Table 7**
Hydrogen-bond geometry (Å, °) for *p*-ClNB at 100 K.

| $D$—H···$A$ | $D$—H | H···$A$ | $D$···$A$ | $D$—H···$A$ |
|---|---|---|---|---|
| C3—H2···O1$^{i}$ | 0.96 (2) | 2.47 (2) | 3.381 (5) | 157.4 (18) |
| C2—H1···O2$^{ii}$ | 0.92 (2) | 2.68 (2) | 3.323 (4) | 127.6 (17) |

Symmetry codes: (i) $-x, -y+1, -z+1$; (ii) $-x+1, y-\frac{1}{2}, -z+\frac{1}{2}$.

The molecule exhibits twofold disorder (50:50 Cl:N occupancy). This disorder persists to low temperature, at least to 100 K. H atoms were located from Fourier difference maps and their fractional coordinates and isotropic displacement parameters were refined.

For all compounds, data collection: *COLLECT* (Nonius, 1998); cell refinement: *SCALEPACK* (Otwinowski & Minor, 1997); data reduction: *DENZO* (Otwinowski & Minor, 1997) and *SCALEPACK*; program(s) used to solve structure: *SHELXS97* (Sheldrick, 2008); program(s) used to refine structure: *SHELXL97* (Sheldrick, 2008); molecular graphics: *SHELXTL-Plus* (Sheldrick, 2008); software used to prepare material for publication: *SHELXL97*.

JMC thanks the Royal Society for a University Research Fellowship and St Catharine's College, Cambridge, for a Senior Research Fellowship. LHT is grateful for PhD funding from the CCLRC *via* the Centre of Molecular Structure and Dynamics and EPSRC grant No. GR/N22403. Mr Andrew Monaghan is thanked for his assistance with thermogravimetric analysis.

**Table 8**
The effect of applying various restraints and constraints.

The restraints were applied such that the N—O distances were approximately equal, as would be expected in a disorder-free system. The N—O distances were restrained to be 1.221 Å, the N—C distances to be 1.47 Å and the C—Cl distances to be 1.74 Å. All bond distances and angles are given in Å and °, respectively.

| | | Restrained | | Constrained | | |
|---|---|---|---|---|---|---|
| | Free refinement | O—N ($\sigma$ = 0.02) | O—N ($\sigma$ = 0.002) | Cl,N—C | N—O | CSD data (average) |
| N1—O1 | 1.300 (7) | 1.279 (7) | 1.240 (4) | 1.156 (6) | 1.240 (4) | 1.221 |
| N1—O2 | 1.179 (7) | 1.201 (7) | 1.240 (4) | 1.157 (6) | 1.222 (4) | 1.221 |
| N1—C1 | 1.330 (6) | 1.323 (6) | 1.319 (6) | 1.465 (6) | 1.326 (5) | 1.467 |
| Cl1—C1 | 1.903 (3) | 1.904 (3) | 1.905 (3) | 1.811 (5) | 1.905 (3) | 1.734 |
| O1—N1—O2 | 124.2 (6) | 124.0 (6) | 124.0 (6) | 138.2 (9) | 124.6 (6) | 115.1† |
| O1—N1—C1 | 113.4 (6) | 114.9 (5) | 117.4 (4) | 110.1 (6) | 116.6 (4) | 118.2 |
| O2—N1—C1 | 122.4 (5) | 121.1 (5) | 118.5 (4) | 111.7 (6) | 118.8 (4) | 118.2 |
| *R* factor | 0.0456 | 0.0464 | 0.0485 | 0.0785 | 0.0480 | – |

† Range of values is markedly broad: 96–129°.

Supplementary data for this paper are available from the IUCr electronic archives (Reference: HJ3058). Services for accessing these data are described at the back of the journal.

**Table 9**
The atomic displacement parameters for the librating group in *p*-ClNB, at selected temperatures, *T* (K), that cover succinctly the full temperature range studied.

| *T* | $U_{ii}$ | C1 | C2 | C3 | Cl1 | O1 | O2 | N1 |
|---|---|---|---|---|---|---|---|---|
| 100 | $U_{11}$ | 0.0226 (9) | 0.033 (1) | 0.030 (1) | 0.0380 (8) | 0.066 (3) | 0.059 (2) | 0.027 (2) |
| 100 | $U_{22}$ | 0.065 (1) | 0.075 (2) | 0.063 (2) | 0.068 (2) | 0.041 (2) | 0.055 (2) | 0.024 (3) |
| 100 | $U_{33}$ | 0.038 (1) | 0.031 (1) | 0.041 (1) | 0.0460 (8) | 0.092 (3) | 0.043 (2) | 0.086 (5) |
| 100 | $U_{eq}$ | 0.0417 (6) | 0.0463 (6) | 0.0448 (6) | 0.0510 (5) | 0.067 (1) | 0.0533 (8) | 0.045 (2) |
| 200 | $U_{11}$ | 0.040 (1) | 0.056 (1) | 0.053 (1) | 0.063 (1) | 0.104 (4) | 0.100 (3) | 0.053 (4) |
| 200 | $U_{22}$ | 0.079 (2) | 0.097 (2) | 0.078 (2) | 0.100 (3) | 0.064 (3) | 0.086 (3) | 0.053 (5) |
| 200 | $U_{33}$ | 0.059 (1) | 0.048 (1) | 0.064 (1) | 0.076 (1) | 0.158 (5) | 0.065 (2) | 0.138 (9) |
| 200 | $U_{eq}$ | 0.0590 (6) | 0.0664 (7) | 0.0645 (7) | 0.0807 (9) | 0.109 (2) | 0.085 (1) | 0.080 (3) |
| 260 | $U_{11}$ | 0.055 (1) | 0.077 (1) | 0.071 (1) | 0.085 (1) | 0.151 (5) | 0.134 (4) | 0.075 (5) |
| 260 | $U_{22}$ | 0.094 (2) | 0.115 (2) | 0.091 (2) | 0.132 (5) | 0.087 (4) | 0.118 (4) | 0.069 (6) |
| 260 | $U_{33}$ | 0.078 (2) | 0.063 (2) | 0.081 (2) | 0.104 (2) | 0.208 (7) | 0.087 (3) | 0.18 (1) |
| 260 | $U_{eq}$ | 0.0752 (8) | 0.0848 (9) | 0.0808 (8) | 0.108 (2) | 0.149 (3) | 0.114 (2) | 0.105 (4) |

## References


Allen, F. H. (2002). *Acta Cryst.* B**58**, 380–388.
Blessing, R. H. (1995). *Acta Cryst.* A**51**, 33–38.
Bruno, I. J., Cole, J. C., Edgington, P. R., Kessler, M., Macrae, C. F., McCabe, P., Pearson, J. & Taylor, R. (2002). *Acta Cryst.* B**58**, 389–397.
Desiraju, G. R. & Steiner, T. (2001). *The Weak Hydrogen Bond in Structural Chemistry and Biology*. New York: Oxford University Press Inc.
González, C. E. & Pusiol, D. J. (1996). *J. Chem. Phys.* **105**, 10776–10781.
Hall, P. G. & Horsfall, G. S. (1973). *J. Chem. Soc. Faraday Trans. 2*, **69**, 1071–1077.
Khotsyanova, T. L., Babushkina, T. A., Kuznetsova, S. I. & Semin, G. K. (1969). *Zh. Strukt. Khim.* **10**, 525–529.
Mak, T. C. W. & Trotter, J. (1962). *Acta Cryst.* **15**, 1078–1080.
Meriles, C. A., Perez, S. C. & Brunetti, A. H. (1996). *Phys. Rev. B*, **54**, 7090–7093.
Meriles, C. A., Perez, S. C., Schurrer, C. & Brunetti, A. H. (1997). *Phys. Rev. B*, **56**, 14374–14379.
Meriles, C. A., Schneider, J. F., Mascarenhas, Y. P. & Brunetti, A. H. (2000). *J. Appl. Cryst.* **33**, 71–81.
Nonius (1998). *COLLECT*. Nonius BV, Delft, The Netherlands.
Otwinowski, Z. & Minor, W. (1997). *Methods in Enzymology*, Vol. 276, *Macromolecular Crystallography*, Part A, edited by C. W. Carter Jr & R. M. Sweet, pp. 307–326. New York: Academic Press.
Sakurai, T. (1962). *Acta Cryst.* **15**, 1164–1173.
Sheldrick, G. M. (2008). *Acta Cryst.* A**64**, 112–122.
Tanaka, I., Iwasaki, F. & Aihara, A. (1974). *Acta Cryst.* B**30**, 1546–1549.
Thomas, L. H. (2007). PhD thesis, University of Cambridge, England.
Thomas, L. H., Welberry, T. R., Goossens, D. J., Heerdegen, A. P., Gutmann, M. J., Teat, S. J., Lee, P. L., Wilson, C. C. & Cole, J. M. (2007). *Acta Cryst.* B**63**, 663–673.
Toussaint, J. (1952). *Mem. Soc. R. Sci. Liege*, **12**, 1–3.